Fibers and Polymers 2005, Vol.6, No.4, 289-296

Degradation and Rheological Properties of Biodegradable Nanocomposites Prepared by Melt Intercalation Method

Su Kyong Lee, Dong Gi Seong, and Jae Ryoun Youn*

School of Materials Science and Engineering, Seoul National University, Seoul 151-742, Korea
(Received February 25, 2005; Revised October 16, 2005; Accepted October 24, 2005)

Abstract: Biodegradable nanocomposites were prepared by mixing a polymer resin and layered silicates by the melt intercalation method. Internal structure of the nanocomposite was characterized by using the small angle X-ray scattering (SAXS) and transmission electron microscope (TEM). Nanocomposites having exfoliated and intercalated structures were obtained by employing two different organically modified nanoclays. Rheological properties in shear and extensional flows and biodegradability of nanocomposites were measured. In shear flow, shear thinning behavior and increased storage modulus were observed as the clay loading increased. In extensional flow, strain hardening behavior was observed in well dispersed system. Nanocomposites with the exfoliated structure had better biodegradability than nanocomposites with the intercalated structure or pure polymer.

Keywords: Nanocomposite, Melt intercalation, Layered silicate, Rheological properties, Biodegradability

Introduction

Nanoclay composites are usually produced by dispersing layered silicates in polymer matrix at nanometer level. Polymer based layered silicate nanocomposites have attracted considerable attention because of their excellent physical properties. Nanocomposites usually exhibit improved properties due to their unique morphology and improved interfacial properties although a small amount of clay is added. They exhibit high tensile strength and modulus, good thermal stability, solvent resistance, flame retardance, improved biodegradability, and decreased gas and liquid permeability. Because these improved properties are obtained when silicate layers are well dispersed in the polymer matrix, it is important to produce well-dispersed system, i.e., exfoliated structure. The polymer-clay nanocomposite, nylon 6 and montmorillonite, was first reported by Toyota research group. Only a small amount of clay loading resulted in significant improvement of thermal and mechanical properties [1]. Numerous research groups have also investigated layered silicate nanocomposites based on a variety of polymers.

Nanocomposites can be prepared by two different methods, the in-situ polymerization [2] and the melt intercalation method. Vaia *et al.* [3] first studied direct intercalation of the layered silicates in polymer melts. Polymers are directly mixed with the clay by using a twin-screw extruder or an internal mixer. If the layer surfaces are sufficiently compatible with the polymer matrix, the polymer can penetrate into the interlayer between clays and expand the gallery spacing. Driving force for insertion of polymer chains into the gallery spacing is shear force. Melt intercalation method is widely used because it is relatively simple, environmentally friendly, and commercially applicable because solvent is not used.

There are two different morphologies in nanoclay/polymer nanocomposites, intercalated and exfoliated (delaminated) structures. These structures can be characterized by small angle X-ray scattering (SAXS) and transmission electron microscope (TEM). Intercalated structure is formed when polymer chains are inserted between the clay layers which are regularly dispersed throughout the composite materials. Exfoliated structure is obtained when clay layers are completely delaminated and individual clay platelets are dispersed on the nanometer scale. SAXS data do not have the characteristic peak in exfoliated structure because the extensive layer separation disrupts the coherent layer stacking. In addition, TEM is generally used to characterize the morphology of the exfoliated nanocomposite by identifying the individual silicate layers.

Biodegradable polymer/layered silicate nanocomposites have been actively investigated recently due to the environmental concerns. The environmental problem of undegradable plastic wastes is growing and alternative disposal methods are limited [4]. Incineration of the plastic wastes always produces a large amount of carbon dioxide and toxic gases, and creates global warming which again contributes to environmental pollution [5]. By these reasons, many researchers are investigating biodegradable nanocomposites that are environmentally friendly and have superior properties to unmodified polymers. There are many studies on biodegradable nanocomposites which are based on poly(ε-caprolactone) (PCL) [6-15], synthetic biodegradable aliphatic polyesters (BAP) [16,17], bacterial poly(3-hydroxybutyrate) (PHB) [18], and polyesteramaide [19]. Mechanical, rheological, and thermal properties of nanocomposites were studied but biodegradation behavior of nanocomposites was not investigated in the studies.

Tetto *et al.* first reported results on the biodegradability of nanocomposites based on PCL. PCL nanocomposites showed improved biodegradability compared with pure PCL due to the catalytic role of organically modified layered silicates in

*Corresponding author: jaeryoun@snu.ac.kr

the biodegradation mechanism, but it was not fully proven [20]. Lee *et al.* reported on the biodegradability of aliphatic polyester (APES) clay nanocomposites. They concluded that retardation of the biodegradability might come from the presence of dispersed silicate layers with large aspect ratios which caused the microorganism to diffuse through more torturous pathways. Therefore, the effective path length and diffusion time for the microorganism were increased and the biodegradation of the APES was hindered [21].

Sinha Ray *et al.* investigated the biodegradability of nanocomposites based on polylactide (PLA). They reported that the presence of terminal hydroxylated edge groups in the silicate layers might be one of the factors responsible for improvement of biodegradability. These hydroxyl groups caused heterogeneous hydrolysis of the PLA matrix after absorbing water from the compost. Due to this type of hydrolysis, the matrix decomposed into very small fragments and eventually disappeared with the compost [4,5,22,23-25]. They also investigated polybutylene succinate (PBS) based nanocomposites that showed improved degradability in the compost. Many cracks appeared in the recovered nanocomposite samples compared with those of neat PBS. The fracture on the surface had advantages for biodegradation because it improved mixing of nanocomposites with the compost, created much larger surface area for further attack by microorganisms [26].

In this study, biodegradable polymer/OMLS (Organically Modified Layered Silicate) nanocomposites were prepared by the melt intercalation. Rheological properties in shear and extensional flows and biodegradability of nanocomposites were investigated as a function of clay loading and degree of dispersion.

Experimental

Materials

A biodegradable polymer under the trade name of GREENPOL from SK Corporation was selected as the matrix resin. It consists of polyethylene (≥67 %), aliphatic polyester (14~17 %) and starch (10~16 %). Two kinds of organically modified layered silicate were used, Cloisite® 15A and Cloisite® 30B, which were supplied by Southern Clay Products, Inc. They were synthesized by replacing Na^+ ions with different organic modifiers.

Preparation of Nanocomposites

Nanocomposites were prepared by the melt intercalation method. Organoclay and polymer chips were premixed by using a mechanical oscillator. The mixture was then dried under vacuum at 80 °C for more than 48 hours. Nanocomposites were melt compounded using a counter-rotating intermeshing twin screw extruder (Brabender PLASTICORDER PLE-651) at barrel temperature of 160 °C and a screw speed of 50 rpm with four different organoclay contents of 1, 3, 5, and 7 wt%.

Characterization

The internal structure of nanocomposites was investigated by using small angle X-ray scattering (SAXS) with the Rigaku Max-3 Cg X-ray diffractometer operated at 40 kV and 35 mA with CuK_α radiation ($\lambda = 0.154184$ nm). The scanned diffraction angle was varied from 0 ° to 12 °. Transmission electron microscope (TEM), Jeol JEM-2000EXII, was used for characterization of the nanocomposite morphology. TEM specimens were cryogenically microtomed to ultra thin sections with the thickness of about 100 nm at −200 °C and coated with carbon for 7 minutes to prevent them from degradation caused by the irradiation of electrons.

The shear and extensional flow behaviors of nanocomposites were examined. Small amplitude oscillatory shear experiments were performed at 160 °C to investigate the linear viscoelastic response of nanocomposites by using RMS from Rheometric Scientific and AR2000 from TA Instruments with the parallel plates of 25 mm in diameter. Constant maximum strain was set to be 5 % and frequency sweep test was conducted from 0.1 s^{-1} to 100 s^{-1}. Dynamic shear measurements of polymer materials are generally achieved by applying a time dependent strain $\gamma(t) = \gamma_0 \sin(\omega t)$, and measuring the resultant shear stress $\sigma(t) = \gamma_0[G'\sin(\omega t) + G''\cos(\omega t)]$, where G' and G" are the storage and loss moduli and γ_0 is an amplitude of shear strain [20].

A uniaxial elongation test at a constant Hencky strain rate was conducted in the melt state by using a Meissner type extensional rheometer commercialized as RME from Rheometric Scientific. Extensional viscosity was measured by applying uniaxial deformation at 160 °C. The sample was placed over a porous metal plate through which nitrogen gas was supplied and the force was measured which uniaxial extension was applied to the specimen with four belts. Extensional viscosity was obtained from the following relationship.

$$\eta_E = \frac{\text{stress}}{\text{extension rate}} = \frac{F(t)}{H_0 W_0 exp[-\dot{\varepsilon}t]\dot{\varepsilon}} \quad (1)$$

where $F(t)$ is measured force, H_0 is thickness of the sample at $t = 0$, W_0 is width of the sample at $t = 0$ and $\dot{\varepsilon}$ is extension rate.

The biodegradability of pure polymer and nanocomposites under the compost was measured at 58 ± 2 °C. Samples had the dimension of 25 × 65 × 1 mm^3. Every ten days the specimens were recovered from the soil, cleansed with isopropyl alcohol, and dried in a vacuum oven. The weight of the dried sample was measured to calculate the residual weight fraction. The average value of three measurements was taken as the result.

Results and Discussion

Structure of Nanocomposites

Figure 1(a) exhibits the SAXS results of Cloisite® 15A and its nanocomposites. 2θ of the nanocomposite was shifted to the lower angle (2.35 °) compared with that of organoclays (2.74 °), but the peak was still identified. So it is believed

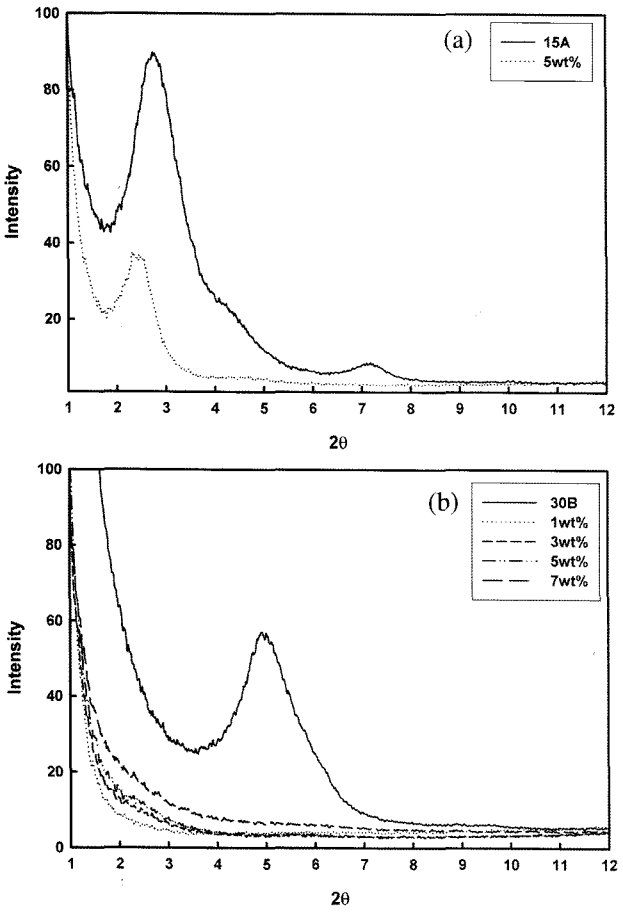

Figure 1. SAXS peaks of nanocomposites: (a) Cloisite® 15A and 5 wt% nanocomposites, (b) Cloisite® 30B and nanocomposites with 1, 3, 5, 7 wt%.

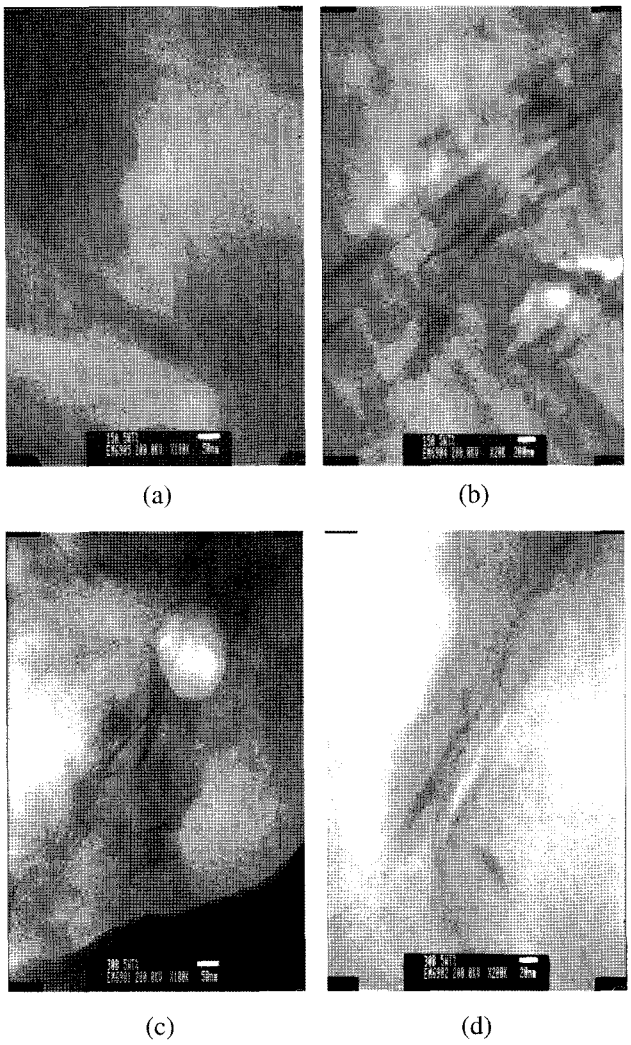

Figure 2. TEM images of nanocomposites: (a) 5 wt% of Cloisite® 15A (×20K), (b) 5 wt% of Cloisite® 15A (×100K), (c) 5 wt% of Cloisite® 30B (×100K), (d) 5 wt% of Cloisite® 30B (×200K).

that interlayer distance between the organoclays was expanded but the typical layered structure was maintained. Figure 1(b) shows the peaks of Cloisite® 30B and its nanocomposites. The clay peak was observed at 4.91 ° corresponding to an interlayer distance of 1.80 nm. But diffraction peaks disappeared in nanocomposites, which means that the exfoliated structure was obtained.

Internal structure of the nanocomposite was observed by taking typical bright field images with a TEM. Dark line represents the clay platelets. Since the silicate layers consist of heavier elements than the interlayer and surrounding polymer matrix, they appear darker in bright field images [22].

Figure 2(a) and (b) represent the TEM images of Cloisite® 15A nanocomposites. In this case, individual silicate layers were stacked together and dispersed in the polymer matrix. It is also clear that Cloisite® 15A nanocomposites had the intercalated structure as mentioned previously from the SAXS result. Figure 2(c) and (d) show TEM images of Cloisite® 30B nanocomposites. Individual clay platelets were dispersed well throughout the polymer matrix and some stacked region also existed. Cloisite® 30B nanocomposites had regions of both intercalated and exfoliated structures.

Rheological Properties

Shear Flow

Figure 3 shows storage moduli of the pure polymer resin and nanocomposites. G' of nanocomposites increased with increasing clay contents and was higher than that of the pure polymer. As the clay content was increased, the increasing rate of G' with respect to the frequency was decreased slightly at low frequencies. This behavior is well known as the solid-like transition. Most polymer nanocomposites showed such behavior [27-32].

Figure 4 shows the storage and loss moduli obtained from frequency sweep test on three different samples. The pure

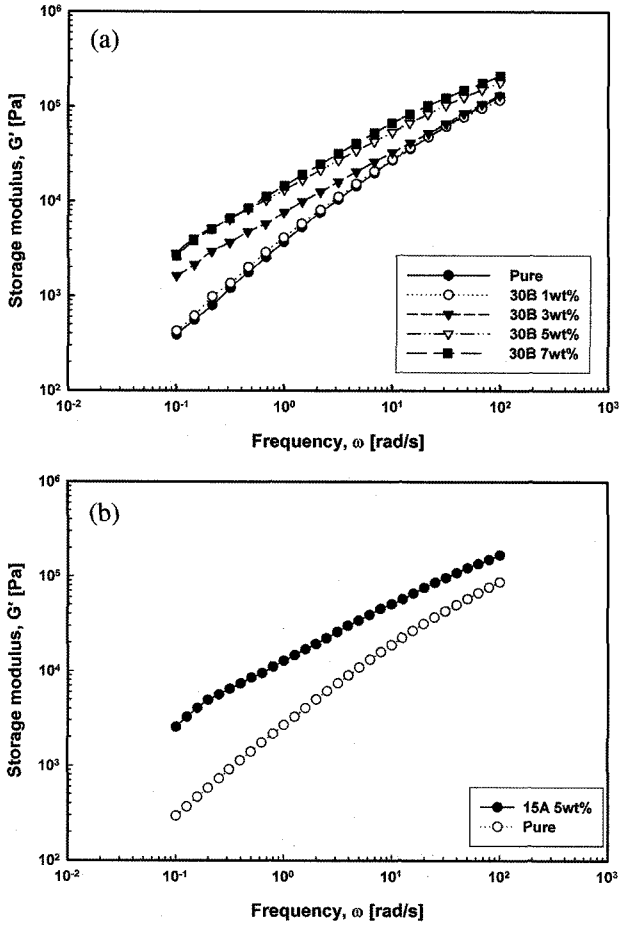

Figure 3. Storage modulus of pure polymer and nanocomposites: (a) nanocomposites with 1, 3, 5, 7 wt% of Cloisite® 30B, (b) nanocomposites with 5 wt% Cloisite® 15A.

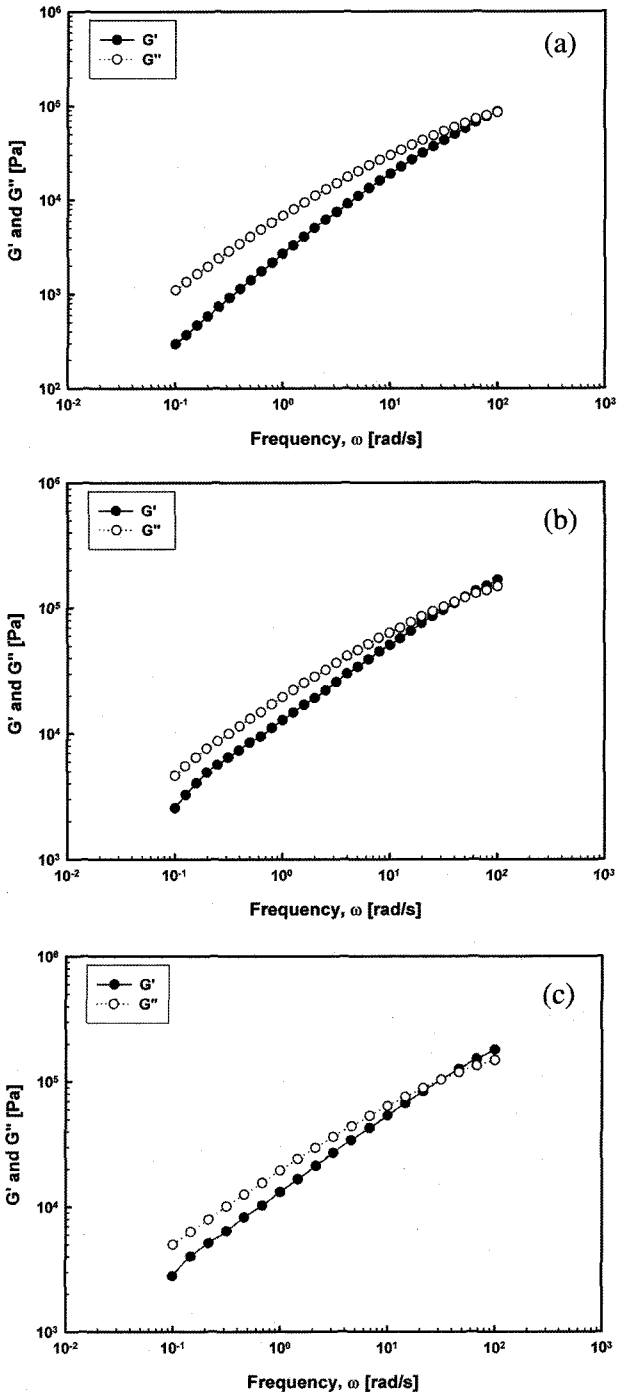

Figure 4. Storage and loss moduli: (a) pure polymer, (b) Cloisite® 15A nanocomposites, (c) Cloisite® 30B nanocomposites.

polymer showed typical viscoelastic behavior, i.e., G' is lower than G". The Cloisite® 15A nanocomposites showed some deviation from the typical behavior. Slopes of G' and G" of the nanocomposites in the terminal zone were less steeper than those of the pure polymer. G' was still lower than G" at lower frequencies and a crossover was observed at 39.81 s^{-1}. Rheological behavior of the Cloisite® 30B nanocomposite was different. At the frequency of 31.62 s^{-1}, the crossover occurred after which G' is higher than G" because nanoclay reinforcing effect in the exfoliated structure is more pronounced than that in the intercalated structure. Similar behaviors were reported in syndiotactic polypropylene nanocomposites [33].

Figure 5 shows shear viscosity of the pure polymer and nanocomposites. The shear viscosity of the nanocomposite was considerably higher than that of the pure polymer at low frequency region and increased with increasing clay loading. There was Newtonian plateau at low shear rate in the pure polymer, but the nanocomposite showed shear thinning behavior even at low frequency region as the clay content increased. At high frequency region, the pure polymer also showed considerable shear thinning.

Figure 6 shows storage modulus and shear viscosity of the pure polymer, Cloisite® 30B, and Cloisite® 15A nanocomposites. Compared with the pure polymer, both nanocomposites had enhanced rheological properties. Cloisite® 30B nanocomposites had slightly higher storage modulus and shear viscosity than

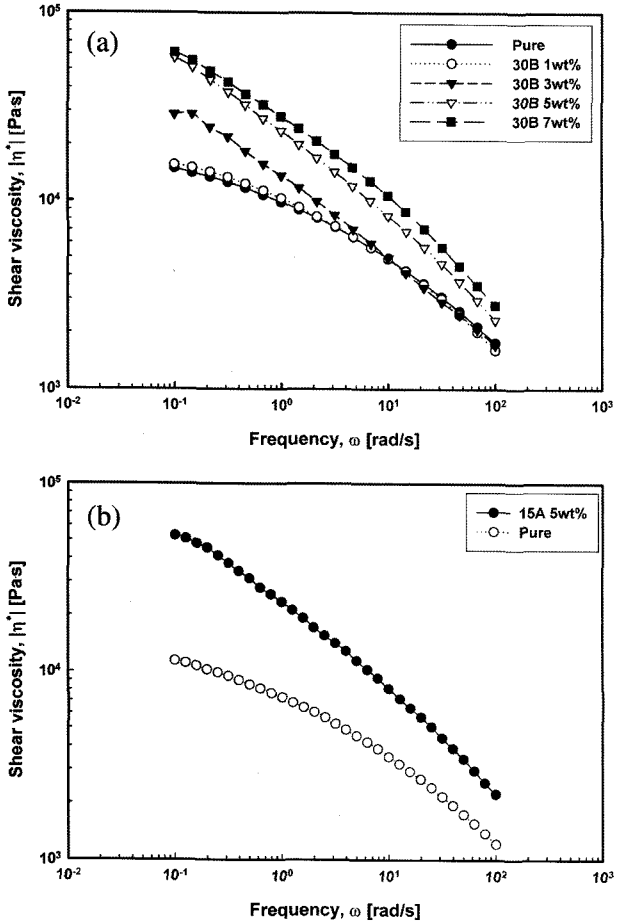

Figure 5. Shear viscosity of pure polymer and nanocomposites: (a) nanocomposites with 1, 3, 5, 7 wt% of Cloisite® 30B, (b) nanocomposites with 5 wt% Cloisite® 15A.

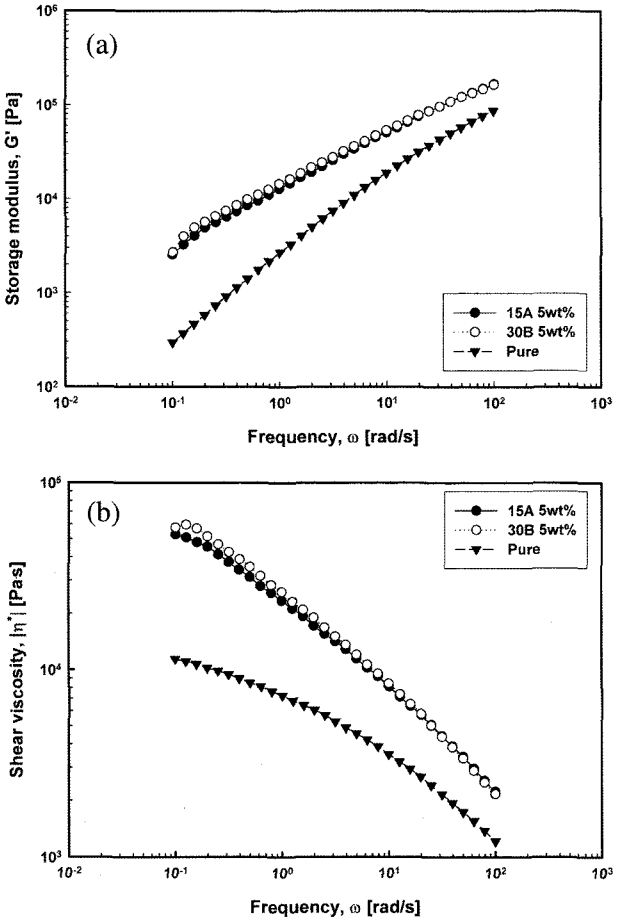

Figure 6. Rheological properties of pure polymer, Cloisite® 30B and Cloisite® 15A nanocomposites with respect to the frequency: (a) storage modulus, (b) shear viscosity.

Cloisite® 15A nanocomposites at low frequency region. Degree of dispersion of the two nanocomposites was different but the rheological behavior in shear flow was not distinguished in between the two systems.

Extensional Flow

Figure 7(a) shows transient extensional viscosity versus time for the pure polymer. Strain hardening behavior was observed, i.e., elongational viscosity increased rapidly with increasing Hencky strain. As the extension rate increased, strain hardening started earlier. Figure 7(b) shows extensional viscosity of the nanocomposite containing 5 wt% of Cloisite® 30B. Degree of strain hardening was slightly decreased for the nanocomposites. This phenomena could be explained by the internal structure of the Cloisite® 30B nanocomposite. It is observed from the SAXS and TEM results that Cloisite® 30B nanocomposites contain both exfoliated and intercalated regions. Partially intercalated or aggregated parts act as weak points. Before strain hardening behavior was observed, samples were broken. In both well-dispersed polyamide 6 and polypropylene nanocomposites, strong strain hardening behavior could be observed [34].

Figure 7(c) shows extensional viscosity of nanocomposites containing 5 wt% of Cloisite® 15A. At low extension rate, weak strain hardening was observed. But as the extension rate increased, strain hardening behavior was not exhibited. In Cloisite® 15A nanocomposites, more weak points exist because degree of dispersion was worse than that of the Cloisite® 30B nanocomposite.

Biodegradability

Figure 8 shows biodegradability of the pure polymer and Cloisite® 30B nanocomposites. Nanocomposites showed much higher biodegradability than the pure polymer and residual weight fraction decreased as the clay loading increased. Sinha Ray *et al.* obtained the same result based on PLA [4,5, 22,35-39] and PBS [26] as mentioned previously. They elucidated that hydroxyl groups in the silicate layers initiated heterogeneous hydrolysis after absorbing water from the compost. Due to the hydrolysis, the matrix decomposed into

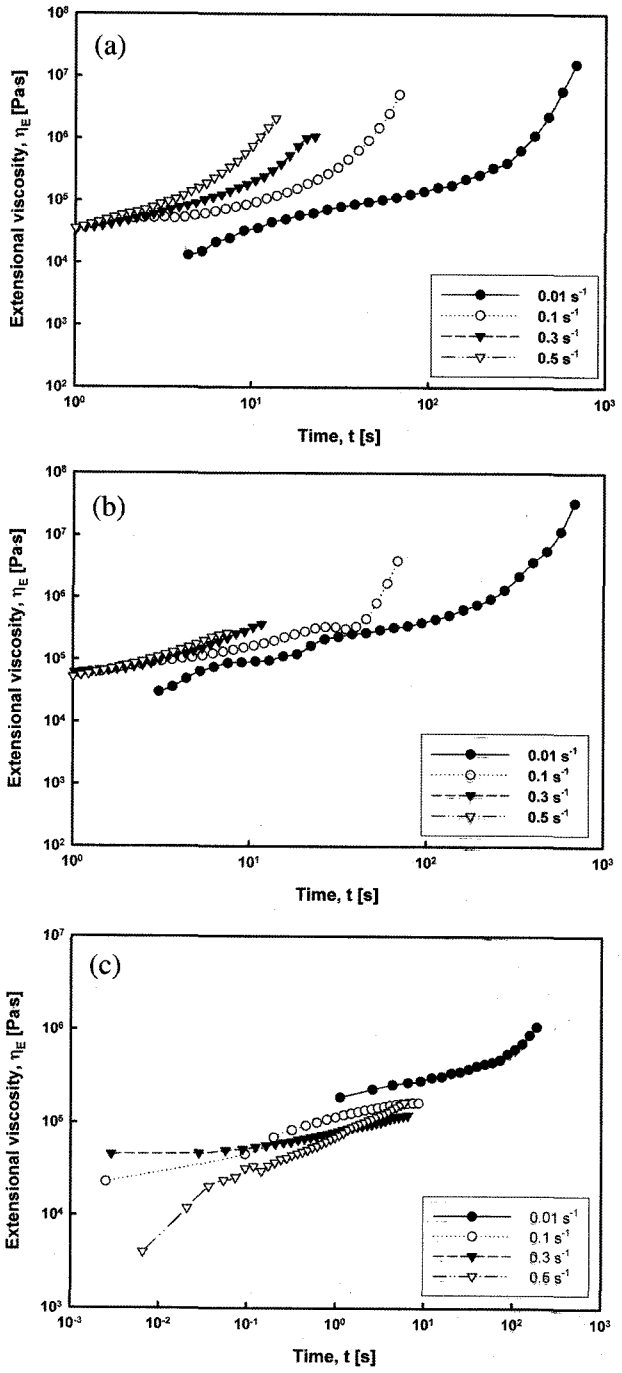

Figure 7. Extensional viscosity at various extension rates: (a) pure polymer, (b) nanocomposites with 5 wt% of Cloisite® 30B, (c) nanocomposites with 5 wt% of Cloisite® 15A.

very small fragments and eventually disappeared with the compost. The reaction needs a certain period of time for beginning and the pure polymer did not show much degradation up to one month. But residual weight fraction of the Cloisite® 30B 7 wt% nanocomposite was higher than those of 3 wt% and 5 wt% nanocomposites. It is believed that when excessive

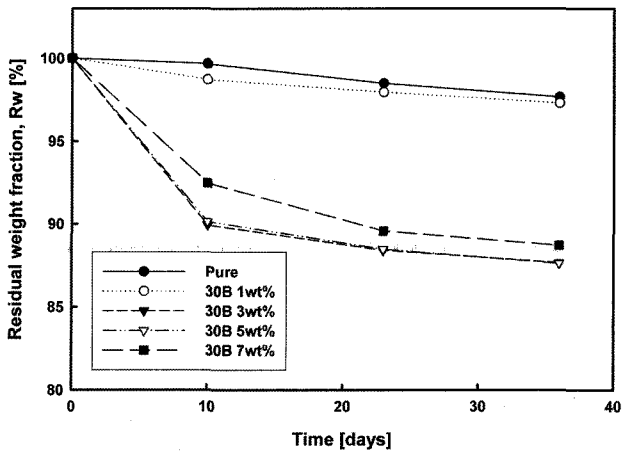

Figure 8. Biodegradability of pure polymer and Cloisite® 30B nanocomposites with respect to clay loading.

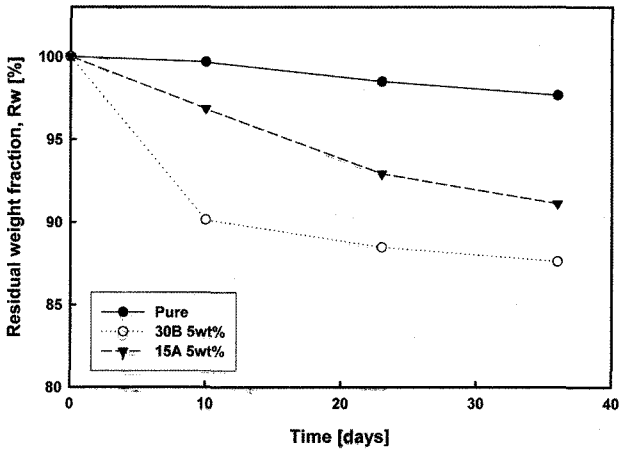

Figure 9. Biodegradability of pure polymer, Cloisite® 30B, and Cloisite® 15A nanocomposites.

clay platelets are dispersed throughout the polymer matrix they act as barriers against water diffusion. Therefore, biodegradability was retarded slightly when 7 wt% of the Cloisite® 30B was included.

Figure 9 shows biodegradability of the pure polymer, Cloisite® 30B 5 wt%, and Cloisite® 15A 5 wt% nanocomposites. Both nanocomposites showed the enhanced biodegradability than the pure polymer and biodegradability of the Cloisite® 30B nanocomposite was higher than the Cloisite® 15A nanocomposite. It may be due to the degree of dispersion and number of terminal hydroxyl groups. Cloisite® 15A nanocomposites have much lower degree of dispersion and do not have hydroxyl end groups. Heterogeneous hydrolysis reaction hardly occurs and attack frequency of the microorganism is lower in the Cloisite® 15A nanocomposite than in the Cloisite® 30B nanocomposite. Biodegradability of the Cloisite® 15A nanocomposite was lower than that of the Cloisite® 30B nanocomposite. As reported for PBS nanocomposites [26],

many cracks appeared in the recovered nanocomposite samples compared with that of neat polymer. The fracture creates larger surface area and makes the microorganism's attack easier.

Conclusions

Nanocomposites based on a biodegradable polymer and layered silicates were prepared via melt intercalation method. By using the small angle X-ray scattering (SAXS) and transmission electron microscope (TEM), internal structure of the nanocomposite was characterized. Cloisite® 30B nanocomposites had both exfoliated and partially intercalated regions and Cloisite® 15A nanocomposites had the intercalated structure. As the clay loading increased, storage modulus was enhanced and solid-like transition was observed. Shear viscosity of the nanocomposite also increased and shear-thinning behavior was observed. In extensional flow, strain hardening behavior was observed in the Cloisite® 30B nanocomposite. Biodegradability of the nanocomposite was also significantly improved. The results were attributed to the difference in the dispersion state of silicate layers depending upon different organoclays.

Acknowledgement

This study was supported by the Korea Science and Engineering Foundation through the Applied Rheology Center (ARC), an officially KOSEF-created engineering research center at Korea University, Seoul, Korea.

References

1. A. Okada, M. Kawasumi, A. Usuki, Y. Kojima, T. Kurauchi, and O. Kamigaito, *MRS Symposium Proceedings*, **171**, 45 (1990).
2. T. J. Pinnavaia and G. W. Beall, "Polymer-Clay Nanocomposites", John Wiley & Sons, 2002.
3. R. A. Vaia, H. Ishii, and E. P. Giannelis, *Chem. Mater.*, **5**, 1694 (1993).
4. S. Sinha Ray, K. Yamada, M. Okamoto, and K. Ueda, *Macromol. Mater. Eng.*, **288**, 203 (2003).
5. S. Sinha Ray, K. Yamada, M. Okamoto, A. Ogami, and K. Ueda, *Chem. Mater.*, **15**(7), 1456 (2003).
6. B. Lepoittevin, M. Devalckenaere, N. Pantoustier, M. Alexandre, D. Kubies, C. Calberg, R. Jérôme, and P. Dubois, *Polymer*, **43**, 4017 (2003).
7. N. Pantoustier, B. Lepoittevin, M. Alexandre, D. Kubies, C. Calberg, R. Jérôme, and P. Dubois, *Polym. Eng. Sci.*, **42**(9), 1928 (2002).
8. N. Pantoustier, M. Alexandre, P. Degée, C. Calberg, R. Jérôme, C. Henrist, R. Cloots, A. Rulmont, and P. Dubois, *e-Polymers*, **009**, 1 (2001).
9. G. Jimenez, N. Ogata, H. Kawai, and T. Ogihara, *J. Appl. Polym. Sci.*, **64**, 2211 (1997).
10. J. Hao, M. Yuan, and X. Deng, *J. Appl. Polym. Sci.*, **86**, 676 (2002).
11. D. Kubies, N. Pantoustier, P. Dubois, A. Rulmont, and R. Jérôme, *Macromolecules*, **35**, 3318 (2002).
12. M. Tortora, V. Vittoria, G. Galli, S. Ritrovati, and E. Chiellini, *Macromol. Mater. Eng.*, **287**, 243 (2002).
13. H. K. Choi, Y. H. Park, S. G. Lyu, B. S. Kim, and G. S. Sur, *Polymer(Korea)*, **23**(5), 724 (1999).
14. Y. Di, S. Iannace, E. D. Maio, and L. Nicolais, *J. Polym. Sci. Part B: Polym. Phys.*, **41**, 670 (2003).
15. K. Okada, T. Mitsunaga, and Y. Nagase, *Korea-Australia Rheology Journal*, **15**(1), 43 (2003).
16. C. H. Lee, S. T. Lim, Y. H. Hyun, and H. J. Choi, *J. Mater. Sci. Lett.*, **22**, 53 (2003).
17. S. T. Lim, C. H. Lee, H. J. Choi, and M. S. Jhon, *J. Polym. Phys.*, **41**, 2052 (2003).
18. S. T. Lim, Y. H. Hyun, C. H. Lee, and H. J. Choi, *J. Mater. Sci. Lett.*, **22**, 299 (2003).
19. M. Krook, A. C. Albertsson, U. W. Gedde, and M. S. Hedenqvist, *Polym. Eng. Sci.*, **42**(6), 1238 (2002).
20. S. Sinha Ray and M. Okamoto, *Prog. Polym. Sci.*, **28**, 1539 (2003).
21. S. R. Lee, H. M. Park, H. Lim, T. Kang, X. Li, W. J. Cho, and C. S. Ha, *Polymer*, **43**, 2495 (2002).
22. S. Sinha Ray, K. Yamada, M. Okamoto, and K. Ueda, *Polymer*, **44**, 857 (2003).
23. S. Sinha Ray, K. Yamada, A. Ogami, M. Okamoto, and K. Ueda, *Macromol. Rapid Commun.*, **23**, 943 (2002).
24. S. Sinha Ray, K. Yamada, M. Okamoto, and K. Ueda, *Nano Lett.*, **2**(10), 1093 (2002).
25. S. Sinha Ray, K. Yamada, M. Okamoto, Y. Fujimoto, A. Ogami, and K. Ueda, *Polymer*, **44**, 6633 (2003).
26. S. Sinha Ray, K. Okamoto, and M. Okamoto, *Macromolecules*, **36**(7), 2355 (2003).
27. R. Krishnamoorti and K. Yurekli, *Current Opinion in Colloid & Interface Science*, **6**, 464 (2001).
28. Y. H. Hyun, S. T. Lim, H. J. Choi, and M. S. Jhon, *Macromolecules*, **34**, 8084 (2001).
29. Y. T. Lim and O. O. Park, *Rheol. Acta.*, **40**, 220 (2001).
30. J. Ren and R. Krishnamoorti, *Macromolecules*, **36**, 4443 (2003).
31. R. Krishnamoorti and E. P. Giannelis, *Macromolecules*, **30**, 4097 (1997).
32. D. Wee, D. G. Seong, and J. R. Youn, *Fibers and Polymers*, **5**(2), 160 (2004).
33. A. Lele, M. Makley, G. Galgali, and C. Ramesh, *J. Rheol.*, **46**(5), 1091 (2002).
34. M. Okamoto, P. H. Nam, P. Maiti, T. Kotaka, N. Hasegawa, and A. Usuki, *Nano Lett.*, **1**(6), 295 (2001).
35. J. H. Chang, Y. U. An, and G. S. Sur, *J. Polym. Sci. Part B. Polym. Phys.*, **41**, 94 (2003).
36. H. J. Kim, M. S. Lee, C. N. Choi, Y. D. Kim, K. Y. Lee and M. B. Ko, *J. Korean Fiber Soc.*, **39**(2), 159 (2002).

37. G. Gorrasi, M. Tortora, V. Vittoria, G. Galli, and E. Chiellini, *J. Polym. Sci. Part B: Polym. Phys.*, **40**, 1118 (2002).
38. B. Lepoittevina, N. Pantoustiera, M. Devalckenaere, M. Alexandre, C. Calberg, R. Jérôme, C. Henrist, A. Rulmont, and P. Dubois, *Polymer*, **44**(7), 2033 (2003).
39. O. Persenaire, M. Alexandre, P. Degée, and P. Dubois, *Biomacromolecules*, **2**, 288 (2001).